UDK 535.37; 661.143

$Y_3Al_5O_{12}$:Re^{3+} (Re=Ce, Eu, and Sm) Nanocrystalline Powders Prepared by Modified Glycine Combustion Method

V. Lojpur, A. Egelja, J. Pantić, V. Đorđević*$^{)}$, B. Matović, M. D. Dramićanin

Vinča Institute of Nuclear Sciences, University of Belgrade, P.O.Box 522, Belgrade, Serbia

Abstract:

Yttrium aluminum garnet doped with rare earth ions (Ce^{3+}, Eu^{3+} and Sm^{3+}) was prepared by modified glycine method. Ce^{3+} as a dopant was used in four different concentrations ($Y_{3-x}Ce_xAl_5O_{12}$; x(%) = 1, 2, 3, 5), while doping concentration of Eu^{3+} and Sm^{3+} was $Y_{3-x}Eu_xAl_5O_{12}$; x(%) = 3 and $Y_{3-x}Sm_xAl_5O_{12}$; x(%) = 1, respectively. Phase composition of powders was investigated using XRD technique and expected target phase was confirmed. Photoluminescent characterization included measurements of excitation and emission spectra, as well as determination of emission decays. $Y_{3-x}Ce_xAl_5O_{12}$ shows intense broad-band emission, with maximum in green spectral region, at about 524 nm under ultraviolet or blue excitation. The origin of the luminescence is the $5d^1{\rightarrow}4f^1$ transition which is both parity and spin allowed. Ultraviolet and blue excitations of Eu^{3+} and Sm^{3+} doped $Y_3Al_5O_{12}$ produce intense orange and red emissions. These emissions are phosphorescent in character and come from spin forbidden f-f electron transitions in Eu^{3+} and Sm^{3+} ions. For the case of Eu^{3+} doping emission comes mainly from $^5D_0{\rightarrow}^7F_1$ transitions with Stark components peaking at 590 nm and 590.75 nm, and with emission decay of 4.15 ms. In the case of Sm^{3+} doping, the emission spectrum, shows $^4G_{5/2}{\rightarrow}^6H_{5/2}$, $^4G_{5/2}{\rightarrow}^6H_{7/2}$, and $^4G_{5/2}{\rightarrow}^6H_{9/2}$ transitions, with the most intense stark components positioned at 567.5 nm, 617 nm, and 650 nm, respectively and for transition centered at 617 nm, emission decay is 3.12 ms.

Keywords: *Yttrium aluminum garnet, Combustion synthesis, Luminescence, Phosphors.*

1. Introduction

Yttrium aluminum garnet ($Y_3Al_5O_{12}$, YAG) together with two more intermediate phases, yttrium aluminum perovskite ($YAlO_3$, YAP) and yttrium aluminum monoclinic ($Y_4Al_2O_9$, YAM) belongs to yttrium aluminum (Y_2O_3-Al_2O_3) system [1, 2]. YAG has good thermal stability (melting point ~1970 ºC), excellent optical and mechanical properties which makes it very suitable for host matrix material [3, 4]. When is doped with trivalent rare earth ions, such as Gd, Eu, Pr, Ce, Tb, it can be widely used in optoelectronic devices [5−9]. Ce-doped YAG (YAG: Ce^{3+}) has numerous applications in solid-state lasers, lighting, plasma display devices, X-ray digital imaging detectors, mammography etc [10−13]. Recently, using of white light emitting diodes (LED) have got considerably attention over conventional light sources, since they possess advantages such as long lifetime, high luminescence efficiency

_____

*$^{)}$ **Corresponding author**: vesipka@vinca.rs

and low power consumption [14]. The 4f-5d transition of YAG: Ce^{3+} efficiently converts blue light from 450 to 470 nm into a very broad band yellow emission in the range of 510 to over 600 nm and represent one of the most popular white LEDs materials [15−17]. Namely, when the yellow photoluminescence is mixed with the exciting blue LED light, emission generates a white output [18]. Orange and red emissions could be obtained by doping YAG with trivalent earth ions such as Eu^{3+} and Sm^{3+} [19,20].

Traditionally, pure yttrium aluminum garnet without intermediate phases was obtained by solid state method at high temperatures over 1600 ºC [21]. However, synthesis at high temperatures produces particles of larger size and irregular morphology which is not favorable in terms of luminescent properties. Since, it is well known that reducing the particle size has a large impact on higher resolution of material, new synthesis techniques were included in the production of this material [22]. In that sense, YAG:Ce^{3+} was obtained *via* numerous soft chemical methods, such as sol-gel, spray pyrolysis, precipitation, hydrothermal/solvothermal synthesis, combustion synthesis and so on [23−27]. Using of this wet methods provide fabrication of controlled size and morphology nano-sized phosphors with advanced photoluminescence properties. Combustion synthesis allows getting particles with narrow size distribution, good crystallinity and no absorbed ligands on the surface of material that are responsible for reducing the efficiency of luminescence.

2. Experimental
2.1. Sample preparation

Modified glycine nitrate combustion method was used for the synthesis of YAG ($Y_3Al_5O_{12}$) powders. Starting chemicals used for the synthesis of rare earth activated YAG powders were Y-nitrate ($Y(NO_3)_3 \cdot 6H_2O$, Aldrich, USA), Al-nitrate ($Al(NO_3)_3 \cdot 9H_2O$, Aldrich, USA), rare earth nitrates ($Ce(NO_3)_3 \cdot 6H_2O$, $Eu(NO_3)_3 \cdot 6H_2O$, and $Sm(NO_3)_3 \cdot 6H_2O$, Aldrich, USA) and glycine (Fischer Scientific, USA). Preparation of $Y_{3-x}Re_xAl_5O_{12}$ powders with rare earth doping concentration x is performed according to the following reaction:

$(3-x)Y(NO_3)_3 \cdot 6H_2O + xRe(NO_3)_3 \cdot 6H_2O + 5Al(NO_3)_3 \cdot 9H_2O + NH_2CH_2COOH$
$\rightarrow Y_{3-x}Re_xAl_5O_{12} + 2CO_2\uparrow + 25NO_2\uparrow + 2.75O_2\uparrow + 65.5H_2O$
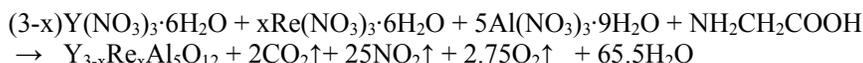
For the synthesis all reactants were first dissolved in distilled water and then poured in to a stainless steel reactor. Reaction was carried out at 500 ˚C for 1h. As prepared powders were additionally annealed at 800 ˚C for 2h, then ground, and again annealed at 950 ˚C for 4h.

2.2. Instruments and measurements

X-ray diffraction (XRD) measurements were performed using Rigaku SmartLab diffractometer. Diffraction data were recorded in a 2θ range from 15 º to 100º, counting for 0.7º / minute in 0.01º steps. Photoluminescence emission and excitation spectra as well as emission decay measurements were done at room temperature on the Fluorolog-3 Model FL3-221 spectroflurometer system (HORIBA Jobin−Yvon). For emission and excitation spectra measurements a 450 W xenon lamp and TBX (HORIBA Jobin−Yvon) detector are used, while for the single photon timing emission decay measurements 150 W pulsed xenon lamp is used, synchronized for the time-correlated single-photon counting (TCSPC).

_____

3. Results and discussion
3.1. X-ray diffraction analysis (XRD)

YAG belongs to the garnet class of oxides whose structure can be represented [28] by coupled octahedrons, tetrahedrons, and dodecahedrons with shared oxygen atoms at the corners, Fig 1. It has a base-centered cubic structure of Ia-3d (O_h^{10}) lattice symmetry with 160 atoms in the cell (80 atoms in the primitive cell). The Y atoms occupy 24(c) sites and they are dodecahedrally coordinated to eight oxygen atoms with D_2 point symmetry, Fig. 2a. The Al atoms occupy the 16(a) sites with octahedral point symmetry C_{3i}, Fig. 2b, and the 24(d) sites with tetrahedral point symmetry S_4, Fig. 2c. The O atoms occupy 96(h) sites.
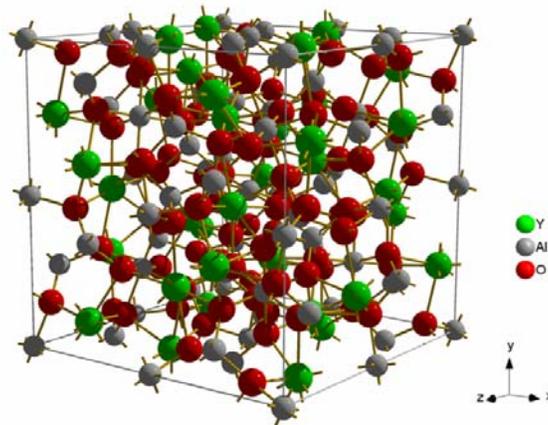
Fig. 1. Schematic representation of $Y_3Al_5O_{12}$ structure.
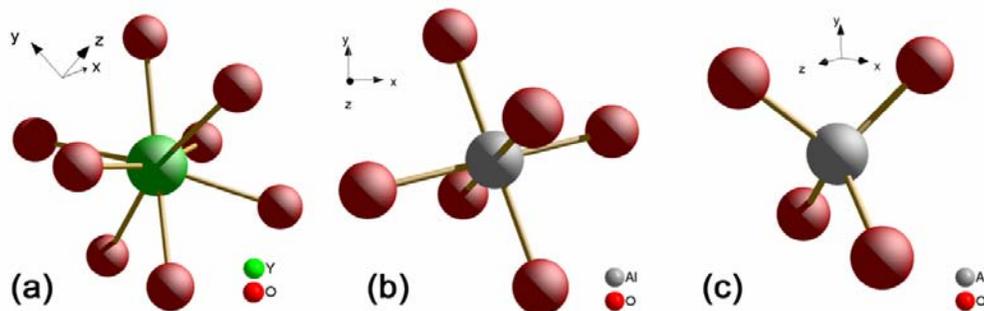
Fig. 2. Cation coordination in $Y_3Al_5O_{12}$: (a) Y dodecahedral coordination, (b) Al-1 octahedral coordination, and (c) Al-2 tetrahedral coordination.

X-ray diffraction (XRD) patterns of rare earth activated YAG powders are shown on Fig 3. All diffraction peaks can be indexed in accordance with PDF 33-0040 card, and no impurity phase peaks are detected. XRD patterns of powders activated with 1 at%, 2 at%, 3 at%, and 5 at% of Ce^{3+}, 3 at% of Eu^{3+}, and 1 at% of Sm^{3+} are given on Fig. 3.

Basic structural parameters of synthesized powders are given in Table 1. The successful incorporation of rare earth atoms in structure is manifested through an increase of lattice unit cell parameter of pure YAG (a= 12.000 Å, PDF 33-0040), which happens because activator ions have larger ionic radii compared to Y^{3+} ($r_{Y(III)}$=0.102 nm, $r_{Ce(III)}$= 0.114 nm, $r_{Eu(III)}$= 0.107 nm, $r_{Sm(III)}$= 0.108 nm) [29]. The crystallite size of about 40 nm is detected in all samples.
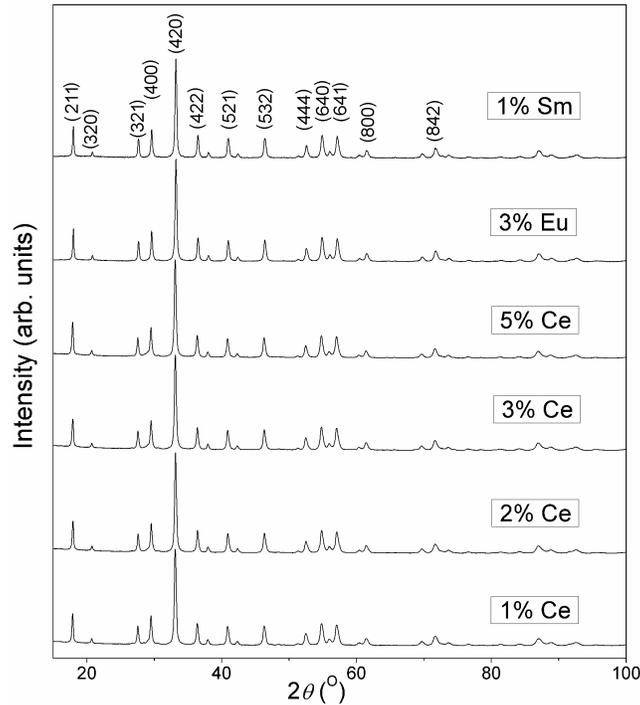
Fig. 3. XRD patterns of $Y_3Al_5O_{12}$ powders activated with diferent % of dopant ions.

Tab. I. Basic structural properties of $Y_3Al_5O_{12}$: Re^{3+} (Re = Ce, Eu, Sm) powders prepared by modified glycine combustion method.

	YAG 1% Ce	YAG 2% Ce	YAG 3% Ce	YAG 5% Ce	YAG 3% Eu	YAG 1% Sm
Lattice parameter, a (Å)	12.0330	12.0466	12.0473	12.0490	12.0450	12.0438
Cell volume (Å³)	1742.3	1748.2	1748.5	1749.2	1748.7	1744.9
Crystallite size (nm)	42.5	33.6	33	33.5	43.18	44.19

3.2. Luminescence properties

Luminescence properties of rare earth activated YAG comes from the intrinsic property of rare earth dopant ion and from the characteristics of the crystallographic site where dopant ion is located. In YAG dodecahedral sites of its structure (Y^{3+} sites) can be partially doped or completely substituted with rare earth cations (Ce^{3+}, Eu^{3+}, Sm^{3+}, etc). This site is centrosymmetric (D_2 point symmetry) with strong crystal field of O^{2-} ions. Ce^{3+} activated YAG provides intense, broad-band visible emission (peaking in the green at about 524 nm) with ultraviolet or blue excitation, Fig. 4a. The origin of the luminescence is the $5d^1 \rightarrow 4f^1$ ($^2D \rightarrow ^2F_J$; J=7/2 and 5/2; the ground state of Ce^{3+} is split into $^2F_{7/2}$ and $^2F_{5/2}$) transition which is both parity and spin allowed with the lifetime of some tens of ns.

Excitation spectra of Ce^{3+} activated YAG for different Ce^{3+} concentrations are presented on Fig. 4b. Due to the crystal field acting on Ce^{3+} ions their 5d electron state is split.

The electron transition occurring at 344 nm comes from the 5d level located slightly below YAG conduction band. Therefore, at the room temperature luminescence is partially quenched and the excitation band is of weak intensity. The main excitation band covers 400 to 500 nm spectral region. This property provides means for fabrication of white light sources using combination of GaN blue LED and Ce^{3+} doped YAG.
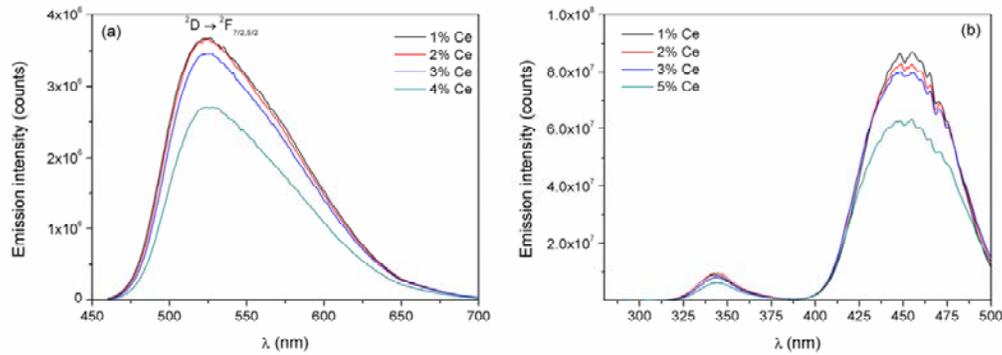
Fig. 4. Photoluminescence spectra of $Y_3Al_5O_{12}$ powders activated with different Ce^{3+} concentrations: (a) emission spectra excited at 450 nm, and (b) excitation spectra monitored at 524 nm.

Ultraviolet and blue excitations of YAG:Eu^{3+} and YAG:Sm^{3+} produce intense orange and red emissions. These emissions are phosphorescent in character and come from spin forbidden f-f electron transitions in Eu^{3+} and Sm^{3+} ions, with decays of several ms. Emission and excitation spectra of YAG:Eu^{3+} are shown on Fig. 5a and b, respectively. Emission spectrum measured with 395 nm excitation, Fig. 5a, shows emission peaks from $^5D_0 \rightarrow {}^7F_J$ (J=0, 1, 2, 3, 4) transitions. When Eu^{3+} ions reside in centrosymmetric sites, like in the case of YAG, the emission comes mainly from $^5D_0 \rightarrow {}^7F_1$ transitions which have magnetic dipole nature. Two Stark components of this transition are located at 590 nm and 590.75 nm, and they are responsible for orange color of YAG:Eu^{3+} emission. The barely visible $^5D_0 \rightarrow {}^7F_0$ transitions at 580 nm further confirms centrosymmetric nature of the Eu^{3+} site. In this type of symmetry this emission should not appear in the spectrum, however, due to J-J mixing very weak emission may be observed.
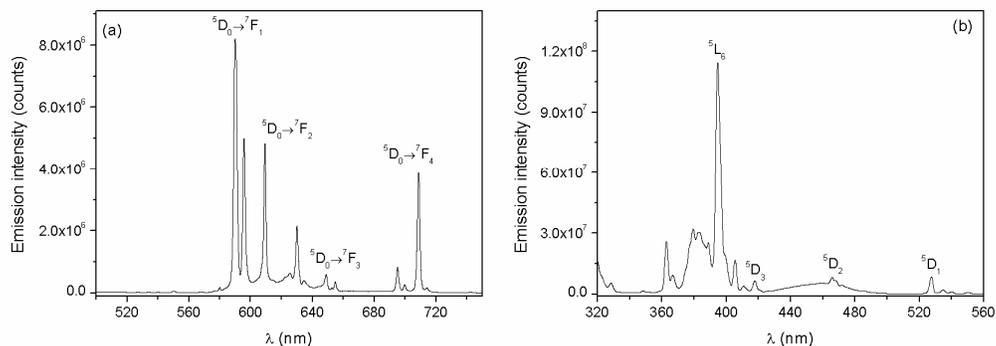
Fig. 5. Photoluminescence spectra of $Y_3Al_5O_{12}$ powders activated with Eu^{3+} ions: (a) emission spectra excited at 395 nm, and (b) excitation spectra monitored at 590 nm.

The other emissions in the spectrum comes from $^5D_0 \rightarrow {}^7F_2$ transition (609.25 nm, 625.25 nm, 630 nm, and 634.5 nm), $^5D_0 \rightarrow {}^7F_3$ transition (648.5 nm, 652.5 nm, and 654.5 nm), and from $^5D_0 \rightarrow {}^7F_4$ transition (695 nm, 699.5 nm, 708.75 nm, and 714 nm). Excitation

spectrum, Fig 5(b), is measured by monitoring emission at 590 nm. The main characteristic Eu^{3+} excitation bands are located at 395 nm ($^5L_6$), 418 nm ($^5D_3$), 466 ($^5D_2$), and 528 nm ($^5D_1$). The emission decay (excitation with 395 nm and detection at 590 nm) showed single exponential behavior with lifetime constant of 4.15 ms.
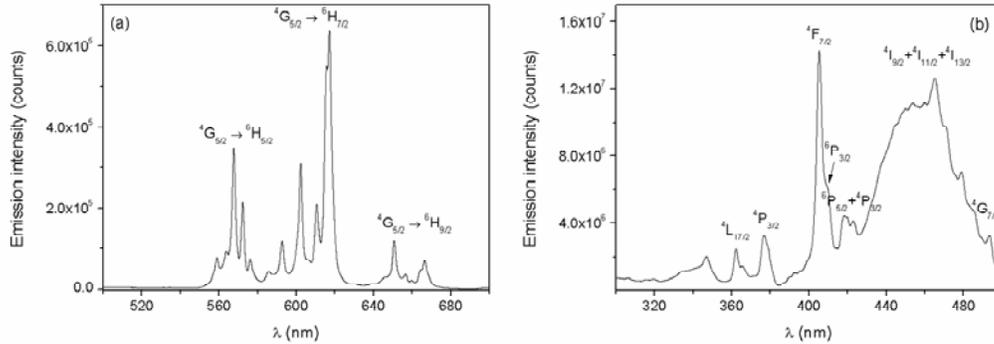
Fig. 6. Photoluminescence spectra of $Y_3Al_5O_{12}$ powders activated with Sm^{3+} ions: (a) emission spectra excited at 405 nm, and (b) excitation spectra monitored at 567.5 nm.

Emission and excitation spectra of YAG:Sm^{3+} are shown on Fig. 6a and b, respectively. The emission spectrum, Fig. 6(a), shows $^4G_{5/2}{\rightarrow}^6H_{5/2}$, $^4G_{5/2}{\rightarrow}^6H_{7/2}$, and $^4G_{5/2}{\rightarrow}^6H_{9/2}$ transitions, with the most intense Stark components positioned at 567.5 nm, 617 nm, and 650 nm, respectively. The main characteristic Sm^{3+} excitation bands, Fig. 6b, are located at 409 nm ($^6P_{3/2}$), 421 nm ($^6P_{5/2}+^4P_{5/2}$), 465 nm ($^4I_{9/2}+^4I_{11/2}+^4I_{13/2}$), and 494 nm ($^4G_{7/2}$). The emission decay (excitation with 405 nm and detection at 617 nm) showed single exponential behavior with lifetime constant of 3.12 ms.

4. Conclusion

Modified glycine method is suitable for simple and cost effective preparation of pure phase yttrium aluminum garnet doped with different rare earth ions (Ce^{3+}, Eu^{3+} and Sm^{3+}). The method provides powders with crystal coherence size of about 40 nm and with complete incorporation of rare earth dopant ions into its structure. After partial substitution of Y^{3+} ions these rare earth ions provide intense luminescence under UV or blue excitation. These emissions are typical for dopant ions and also reflect centrosymmetry of the crystallographic site where they are introduced. Both parity and spin allowed $5d^1{\rightarrow}4f^1$ transition of Ce^{3+} ions provide intense, broad green emission with also broad excitation band spanning from 400 nm to 500 nm, which is extremely useful for preparation of white light sources. Ultraviolet and blue excitations of YAG:Eu^{3+} and YAG:Sm^{3+} produce intense orange and red emissions and these emission are phosphorescent in character since they origin from spin forbidden f-f electron transitions. These characteristics show that modified glycine method provide YAG:Eu^{3+} and YAG:Sm^{3+} powders suitable for phosphor applications. The small crystallite size makes these powders attractive for use as precursors for preparation of YAG transparent ceramics.

Acknowledgements

5. References

1. W. Gao, Y. Hu, W. Zhuang, S. Zhang, Y. Liu, H. He: J. Rare Earth. 27 (2009) 886
2. H. Yang, G. Zhu, L. Yuan, C. Zhang, F. Li, H. Xu, A. Yu: J. Am. Ceram. Soc. 95 (2012) 49
3. Y. Zorenko, T. Voznyak, V. Gorbenko, E. Zych, S. Nizankovski, A. Danko, V. Puzikov: J. Lumin. 31 (2011) 17
4. N. Jia, X. Zhang, W. He, W. Hu, X. Meng, Y. Du: J. Alloy. Compd. 509 (2011) 1848
5. H. Yang, Y.S. Kim: J. Lumin. 128 (2008) 1570
6. G. Blasse, A. Bril: Appl. Phys. Lett. 11 (1967) 53
7. H. Yung, D.K. Lee, Y.S. Kim: Mater. Chem. Phys. 114 (2009) 665
8. A. Potdevin, B. Caillier, G. Chadeyron, D. Boyer, R. Mahiou: J. Phys. D Appl. Phys. 38 (2005) 3251
9. L. Wang, L. Zhang, Y. Fan, J. Luo, P. Zhang, L. An: J. Am. Ceram. Soc. 89 (2006) 3570
10. M. K. Ashurov, A. F. Rakov, R. A. Erzin: Solid State Commun. 120 (2001) 491
11. S. Lee, S. Y. Seo: J. Electrochem. Soc. 149 (2002) 85
12. T. Kojima, in: S. Shionoya, W.M. Yen (Eds.), Phosphor Handbook, CRC Press, New York (1998) 628
13. S.L. David, C.M. Michail, M. Roussou, E. Nirgianaki, A.E. Toutountzis, I.G. Valais, G. Fountos, P.F. Liaparinos, I. Kandarakis, G. Panayiotakis: IEEE Trans. Nucl. Sci. 57 (2010) 951
14. Y. Li, R. M. Almeida: J. Phys. D Appl. Phys. 46 (2013) 165102
15. W. H. Chao, R. J. Wu, T. B. Wu: J. Alloy. Compd. 506 (2010) 98
16. L. Mančić, K. Marinković, B. A. Marinković, M. Dramićanin, O. Milošević: J. Eur. Ceram. Soc. 30 (2010) 577
17. S. Nishiura, S. Tanabe, K. Fujioka, Y. Fujimoto: Opt. Mater. 33 (2011) 688
18. Z. Zhou, S. Liu, F. Wang, Y. Liu: J. Phys. D Appl. Phys. 45 (2012) 195105
19. S. Ćulubrk, V. Lojpur, V. Đordjević, M. D. Dramićanin, Sci. Sint. 45 (2013) 323
20. R. Krsmanović, Ž. Antić, I. Zeković, B. Bártová, M. D. Dramićanin, Radiat. Meas. 45 (2010) 438
21. S. A. Hassanzadeh-Tabrizi: Adv. Powder Technol. 23 (2012) 324
22. Y. H. Song, T.Y. Choi, T. Masaki, K. Senthil, D. H. Yoon: Curr. Appl. Phys. 12 (2012) 479
23. P. F. S. Pereira, J. M. A. Caiut, S. J. L. Ribeiro, Y. Messaddeq, K. J. Ciuffi, L. A. Rocha, E. F. Molina, E. J. Nassar: J. Lumin. 126 (2007) 378
24. Y. H. Zhou, J. Lin, M. Yu, S. M. Han, S. B. Wang, H. J. Zhang: Mater. Res. Bull. 38 (2003) 1289
25. H. M. H. Fadlalla, C. C. Tang: Mater. Chem. Phys. 114 (2009) 99
26. Z. Wu, X. Zhang, W. He, Y. Du, N. Jia, G. Xu: J. Alloy. Compd. 468 (2009) 571
27. F. Yen-Pei, W. Shaw-Bing, H. Chin-Shang: J. Alloy. Compd. 458 (2008) 318
28. Y-N. Xu, W. Y. Ching: Phys. Rev. B 59 (1999) 10530
29. John A. Dean: Lange's Handbook of Chemistry, McGraw-Hill, New York (1999) 4.30

Садржај: *Итријум алуминијум гарнет допиран јонима ретких земаља (Ce^{3+}, Eu^{3+} и Sm^{3+}) синтетисан је сагоревањем модификованог прекурсорског раствора нитрата којем је додат глицин. Јон Ce^{3+} је као допант коришћен са четири различите концентрације ($Y_{3-x}Ce_xAl_5O_{12}$; $x(\%) = 1, 2, 3, 5$), док су концентрације јона Eu^{3+} и Sm^{3+} биле $Y_{3-x}Eu_xAl_5O_{12}$; $x(\%) = 3$ and $Y_{3-x}Sm_xAl_5O_{12}$; $x(\%) = 1$, респективно. Очекивани фазни*

састав прахова потврђен је XRD анализом. Фотолуминесцентна карактеризација је укључивала мерења ексцитационих и емисионих спектара, као и одређивање времена живота. $Y_{3-x}Ce_xAl_5O_{12}$ карактерише широка интензивна емисија са максимумом у зеленој области, на око 524 nm, након побуђивања у ултраљубичастој или плавој области. Луминесценција потиче од $5d^l{\rightarrow}4f^l$ прелаза који је дозвољен и по парности и по спину. Побуђивање $Y_3Al_5O_{12}$ допираног јонима Eu^{3+} и Sm^{3+} производи интензивну наранџасту и црвену емисију. Ове емисије су фосфоресцентног карактера услед f-f прелаза електрона који је спински забрањен код јона Eu^{3+} и Sm^{3+}. У случају допирања јонима Eu^{3+} емисија потиче углавном од $^5D_0{\rightarrow}^7F_1$ прелаза где Штаркове компоненте имају максимуме на 590 nm и 590.75 nm, дајући време живота од 4,15 ms. У случају допирања јонима Sm^{3+} емисиони спектар карактеришу прелази $^4G_{5/2}{\rightarrow}^6H_{5/2}$, $^4G_{5/2}{\rightarrow}^6H_{7/2}$ и $^4G_{5/2}{\rightarrow}^6H_{9/2}$, где су максимуми Штаркових компонената позиционирани на 567.5 nm, 617 nm и 650 nm, респективно, а прелаз позициониран на 617 nm има време живота 3,12 ms.

Кључне речи*: Итријум алуминијум гарнет, синтеза сагоревањем, луминесценција, фосфорни материјали.*